Organic Electronics 13 (2012) 1340–1348

Contents lists available at SciVerse ScienceDirect

Organic Electronics

journal homepage: www.elsevier.com/locate/orgel

Improving color stability of blue/orange complementary white OLEDs by using single-host double-emissive layer structure: Comprehensive experimental investigation into the device working mechanism

Yongbiao Zhao, Liping Zhu, Jiangshan Chen *, Dongge Ma *

State Key Laboratory of Polymer Physics and Chemistry, Changchun Institute of Applied Chemistry, Graduate School of Chinese Academy of Sciences, Chinese Academy of Sciences, Changchun 130022, People's Republic of China

ARTICLE INFO

Article history:
Received 29 October 2011
Received in revised form 9 April 2012
Accepted 18 April 2012
Available online 3 May 2012

Keywords:
Organic light emitting diode
Color stability
Double emissive layer
White

ABSTRACT

In this paper, we successfully improved the spectral stability in blue/orange complementary white organic light-emitting diodes (OLEDs) by utilizing hole-type single host double emissive layer structure. The demonstrated double emissive layer structure effectively suppresses the direct recombination of electron–hole pairs on the hole-trapping orange phosphor and thus reduces the deteriorated effect of charge trapping on electroluminescence spectrum stability by controlling exciton recombination zone. It is shown that the white light emission is a cascade energy transfer process from host to blue phosphor and then to orange phosphor, which seems to be less affected by the driving conditions. Thus, the change in Commission Internationale de L'Eclairage coordinates (CIE) in the white OLEDs is less than (±0.010, ±0.007) as the voltage increases from 4 V to 9 V, which correspond to the luminance increasing from 200 cd m^{-2} to about 20,000 cd m^{-2}. This is superior to that of co-doped single emissive layer devices, which show much larger CIEs variation of (±0.05, ±0.02) in the same driving voltage range. We gave detailed analysis on the exciton recombination processes and well elucidated the working mechanism of the fabricated double emissive layer structure white OLEDs.

© 2012 Elsevier B.V. All rights reserved.

1. Introduction

Organic light-emitting diodes (OLEDs) [1] with white emission spectra are promising candidates for future lighting sources [2–5]. They potentially offer high efficiency and excellent color quality, allowing for substantially lower power consumption for lighting applications compared to traditional lighting sources. Recent advances have greatly improved the performance of white OLEDs, and today's state-of-the-art white OLEDs can even beat the fluorescent tube in efficiency [6,7].

It was known that due to their high-lying highest occupied molecular orbital (HOMO) and/or low-lying lowest unoccupied molecular orbital (LUMO) than host materials, most guest dyes, especially red and green, in host–guest systems can trap holes and/or electrons [8–14]. Charge trapping can lead to direct recombination of holes and electrons on guests, which is beneficial to eliminate the energy losses of energy transfer from hosts to guests, thus realizing high efficiency [5,11,15]. It was found recently that a limited charge trapping effect in fluorescent host/guest systems by the guest leads to a higher OLED electroluminescence efficiency, a phenomenon attributed to the role of triplet–triplet annihilation (TTA) in converting triplet excitons into additional singlet excitons [16].

Actually, the charge trapping was also reported to have a deteriorated effect on the color stability of white OLEDs with multi-doped single emitter [14,17,18]. It can be calculated that the charge carrier trapping rate τ^{-1} would

* Corresponding authors.
E-mail addresses: jschen@ciac.jl.cn (J. Chen), mdg1014@ciac.jl.cn (D. Ma).

1566-1199/$ - see front matter © 2012 Elsevier B.V. All rights reserved.
http://dx.doi.org/10.1016/j.orgel.2012.04.015

change with the driving voltages, which can be written as [17]:

$$\tau^{-1} = \frac{D}{L_T^2} + \frac{\mu}{L_T}\frac{U - U_0}{d}, \quad (1)$$

where D is the diffusion coefficient of the charge carriers, μ is the charge carrier mobility, L_T is the average distance a charge travels before reaching a trapping center, d is the emitter thickness, U is the voltage applied to the device and U_0 is the built-in field. The estimated transit rate $\tau_{Transit}^{-1}$ (the inverse of the average time it takes for a charge to transit through the emitter) can be expressed as:

$$\tau_{Transit}^{-1} = \frac{\mu(U - U_0)}{d^2}. \quad (2)$$

Then the ratio of the trapping rate τ^{-1} and the transit rate $\tau_{Transit}^{-1}$ is in the form of:

$$q(U) = \frac{\tau^{-1}}{\tau_{Transient}^{-1}} = \frac{D}{\mu}\left(\frac{d}{L_T}\right)^2 \frac{1}{U - U_0} + \frac{d}{L_T}. \quad (3)$$

This indicates that $q(U)$ is inversely proportion to U. As $q(U)$ is proportional to the ratio between the emission intensity of guest based on charge carrier trapping (and then direct electron/hole recombination) and that based on energy transfer, so the ratio between the emission intensity of different guests is also inversely proportion to U, which is the criminal for color instability. For the problem of spectral change due to charge carrier trapping effect, Wang et al. [14,18] gave experimental examples in their white OLEDs, where two phosphorescent dyes, namely, iridium(III)[bis(4,6-difluorophenyl)-pyridina-to-N,C20]-picolinate (FIrpic) for blue emission and bis(2-(9,9-diethyl-9H-fl-uoren-2-yl)-1-phenyl-1H-benzoimidazol-N,C3)iridium(acetylacetonate) ((fbi)$_2$Ir(acac)) for orange emission, into 1,3-bis(9-carbazolyl)benzene (mCP) or 4,4′,4″-tri(N-carbazolyl)triphenylamine (TCTA) as the emission layer (EML). They have well explained the spectral instability by the hole trapping effect of (fbi)$_2$Ir(acac) in emissive layer.

With respect to the doped single emissive layer structures, the bi- [10] or multi-emissive layer [7,19–21] structures seem to relatively stabilize the electroluminescent spectrum of the fabricated white OLEDs. Though they did not give detailed analysis on why these devices can keep constant Commission Internationale de L'Eclairage coordinates (CIEs), it shed light on that color-stable white OLEDs featured multi-emission layer structure. Recently, Hsiao et al. demonstrated [22] that by putting the charge carrier trapping dopant outside the recombination zone and thus preventing the direct exciton formation on these dopants, it is possible to suppress the poor color stability generally observed in white OLEDs. This seems to be a controllable method to realize color stable white OLEDs.

In this paper, we fabricated double EML structure white OLEDs and found that the spectral stability of the resulting white OLEDs is greatly improved, which showed CIEs variation less than (0.010, 0.007) as the driving voltages increase from 4 V to 9 V. This is realized by controlling the exciton recombination region within the blue phosphorescent EML and thus preventing direct electron–hole recombination on the orange emitting dopants. The detailed electrical and optical analysis clearly showed that energy transfer is the main working mechanism for the orange emission from (fbi)$_2$Ir(acac) and the blue emission from FIrpic, which seems to be less affected by the driving voltage. And we also found that the width of the exciton recombination zone in our white OLEDs is less than 3 nm, which is the key parameter to the device design.

2. Experimental

The fabricated devices were grown on cleaned glass substrates pre-coated by a 180 nm thickness of ITO with a sheet resistance of 10 Ω per square. The ITO surface was treated by oxygen plasma for 2 min, following a degrease in an ultrasonic solvent bath, and then was dried at 120 °C before loaded into an evaporator. All layers were grown by thermal evaporation in a high-vacuum system with a pressure of less than 5×10^{-4} Pa without breaking the vacuum. The various device structures were described in the text. For the case of doping, the deposition rates of both host and guest were controlled with their correspondingly independent quartz crystal oscillators. The evaporation rates were monitored by a frequency counter and calibrated by a Dektak 6M profiler (Veeco). The overlap between ITO and Al electrodes was 4 mm × 4 mm which is the active emissive area of the devices. The current–voltage–brightness characteristics were measured by using a set of Keithley source measurement units (Keithley 2400 and Keithley 2000) with a calibrated silicon photodiode. The electroluminescence (EL) spectra were measured by a Spectrascan PR650 spectrophotometer. All the measurements were carried out in ambient atmosphere at room temperature.

The samples for transient photoluminescence (PL) measurements were prepared on SiO_2 wafer. The samples were excited by a Quanty-ray DCR-2 pulsed Nd:YAG laser with THG (third harmonic generation) 355 nm output and ca. 3 ns pulse width. Transient PL signals were then collected and transformed to electrical signal by a photomultiplier tube (PMT) after filtered by a monochromator. The final results were then displayed on an oscilloscope (Agilent Model 54825A, 500 MHz/2 Gs/s). The PL lifetimes were then obtained by an exponential fit of emission decay curves.

3. Results and analysis

3.1. Performance comparison of single EML and double EML white OLEDs

The fabricated single and double EML structure white OLEDs in our study are ITO/MoO_3 (10 nm)/NPB (80 nm)/TCTA (5 nm)/TCTA: 8 wt.% FIrpic: 1 wt.% (fbi)$_2$Ir(acac) (10 nm)/TPBi (50 nm)/LiF (1 nm)/Al (150 nm) and ITO/MoO_3 (10 nm)/NPB(80 nm)/TCTA (5 nm)/TCTA: 6 wt.% (fbi)$_2$Ir(acac) (5 nm)/TCTA: 8 wt.% FIrpic (5 nm)/TPBi (50 nm)/LiF (1 nm)/Al(150 nm), respectively. It should be mentioned that the concentration of (fbi)$_2$Ir(acac) in the single EML device must be less than 1.25 wt.% in order to get an accepted white emission. However, it can be seen

that the concentration of $(fbi)_2Ir(acac)$ in the double EML device is much higher, making the controlling of doping concentration more easily. In our devices, TCTA with a triplet energy of 2.82 eV, which is higher than that of FIrpic (2.65 eV) and $(fbi)_2Ir(acac)$ (2.22 eV), is selected as the host material. From the large difference between hole mobility (about 3×10^{-4} cm^2 V^{-1} s^{-1} at 0.5 MV cm^{-1}) and electron mobility (<10^{-8} cm^2 V^{-1} s^{-1}) of TCTA [23,24], it can be concluded that the recombination zones in both white OLEDs are suited at the vicinity of the interface between the EML and TPBi. And the incorporated FIrpic may move the recombination zones further into the EML [25] due to the dominant electron transporting property of FIrpic [14] and the small LUMO level difference of FIrpic with respect to TPBi (FIrpic LUMO is 3.0 eV, TPBi LUMO is 2.9 eV). To effective block excitons in recombination region, 5 nm TCTA between NPB and EML is used.

Fig. 1(a) shows the current density–voltage (J–V) and luminance–voltage (L–V) curves of the two white OLEDs. It can be seen that they show approximate properties of J–V and L–V, indicating that the difference of EML structure does not significantly change the transport and recombination properties of the charge carriers in the EMLs. Of course, although the improvement is not very large, it is clear that the efficiency at higher luminance in the double EML white OLED is higher than that in the single EML white OLED, as shown in Fig. 1(b). This indicates that the charge carrier recombination in the double EML white OLED should be further effective than that in the single EML white OLED. This should also be identical to the fact that, as shown in Fig. 2(b and d), the single EML white OLED shows larger increment at wavelength around 410 nm, which is much possibly from the emission of the electron transporting material TPBi (see Section 1, Supporting information), at high voltages compared with the double EML white OLED.

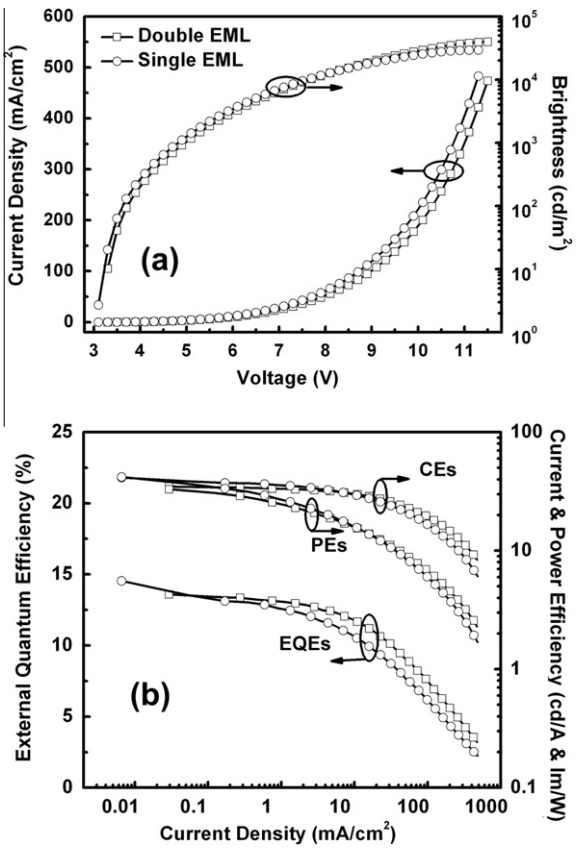

Fig. 1. (a) Voltage–current–luminance curves and (b) EQE & PE & CE vs. current density curves of single EML white OLED (circle) and double EML white OLED (square).

The EL spectra of the two devices at different driving voltages are shown in Fig. 2(a and c). It can be seen that as the driving voltage increases from 4 V to 9 V, the blue to orange emission ratio in the single EML white OLED shows a pronounced change, which is the same case as that in Wang's white OLEDs [14,18]. However, it is clear that the double EML white OLED keeps almost unvaried spectra with voltages. Fig. 3 shows the CIE behaviors of the two devices at different driving voltages. The CIE of the single EML white OLED changes from (0.417, 0.469) at 4 V to (0.362, 0.448) at 9 V, whereas the CIE variation in the double EML white OLED is only (0.010, 0.007) from (0.308, 0.426) at 4 V to (0.318, 0.433) at 9 V. Obviously the spectral stability of the double EML white OLED is greatly improved relative to the single EML white OLED. The higher efficiency, reduced efficiency roll-off and improved color stability in the double EML devices indicate that the double EML white OLED should have different EL processes from the single EML white OLED.

3.2. Energy transfer processes

It was reported that energy transfer would affect the exciton lifetime [26]. If the energy transfer from the donor to acceptor occurs, the lifetime of the donor would decrease. To examine the energy transfer processes in our double EML white OLEDs, the transient PL [27] behaviors of two films with composition of quartz/TCTA: 8 wt.% FIrpic (4 nm) (Film 1) and quartz/TCTA: 8 wt.% FIrpic (4 nm)/TCTA: 8 wt.%$(fbi)_2Ir(acac)$ (4 nm) (Film 2) are investigated. The transient PL decay curves of the two films monitored at 480 nm (emission of FIrpic) are shown in Fig. 4. As can be seen, the lifetime of Film 1 is fitted to be about 0.91 μs. However, the lifetime in Film 2 is decreased to about 0.43 μs. If not considering TTA, the lifetime of triplet excitons on FIrpic in Film 1 can be expressed as:

$$\tau_1 = 1/(\kappa_R + \kappa_{NR}), \quad (4)$$

where κ_R and κ_{NR} are the rate constants of the radiative and non-radiative processes. However, in Film 2, as the 4 nm TCTA: 8 wt.%$(fbi)_2Ir(acac)$ layer is deposited on TCTA: 8 wt.% FIrpic, the energy transfer from FIrpic to $(fbi)_2Ir(acac)$ should be considered and the lifetime of triplet excitons on FIrpic in Film 2 can then be written as:

$$\tau_2 = 1/(\kappa_R + \kappa_{NR} + \kappa_{ET}), \quad (5)$$

where κ_{ET} is the rate constant of the energy transfer from FIrpic to $(fbi)_2Ir(acac)$. From Eq. (4) and (5), we can derive the energy transfer efficiency as:

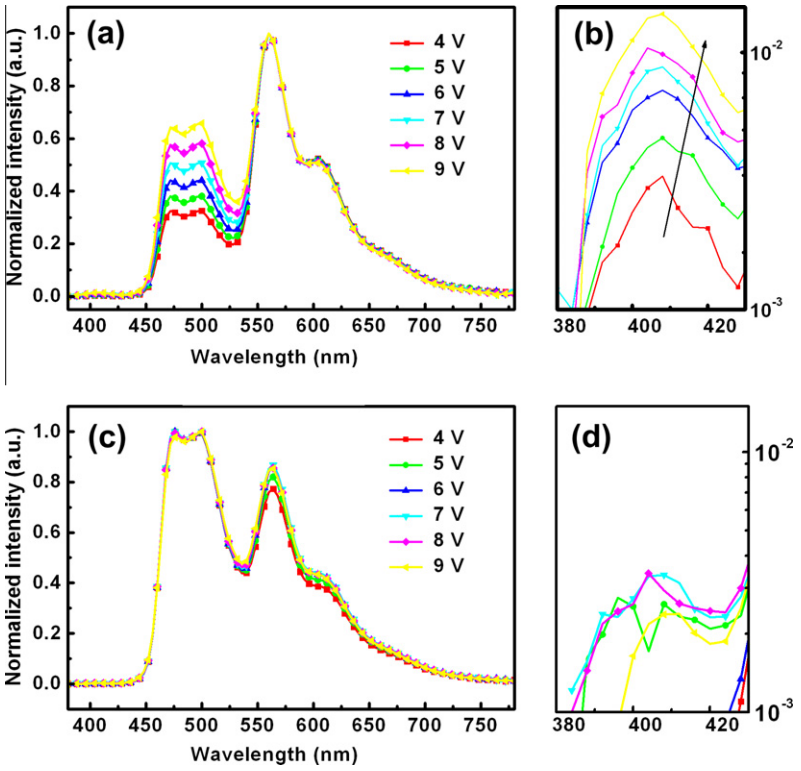

Fig. 2. EL spectra of single EML and double EML white OLEDs at different driving voltages.

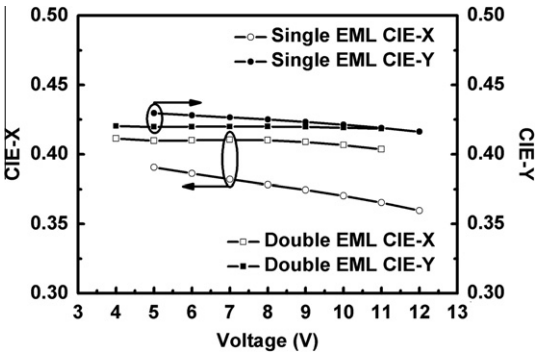

Fig. 3. CIE variations of single EML (circle) and double EML (square) white OLEDs at different driving voltages.

$$\eta_{ET} = \kappa_{ET}/(\kappa_R + \kappa_{NR} + \kappa_{ET}) = 1 - \tau_2/\tau_1 = 52.7\%. \quad (6)$$

This means that there exists a strong energy transfer between the TCTA: 8 wt.% FIrpic layer and the TCTA: 8 wt.%$(fbi)_2Ir(acac)$ layer in Film 2 and more than half triplet excitons in TCTA: 8 wt.% FIrpic layer are transferred to TCTA: 8 wt.% $(fbi)_2Ir(acac)$ layer. This also indicates that there should be a strong energy transfer between the orange EML and the blue EML in our double EML white OLED. Also shown is the PL transient decay curves of quartz/TCTA: 8 wt.% $(fbi)_2Ir(acac)$(4 nm) (Film 3). As can be seen, the transient PL signal of Film 3 monitored at 560 nm, which corresponding to the emission from $(fbi)_2Ir(acac)$,

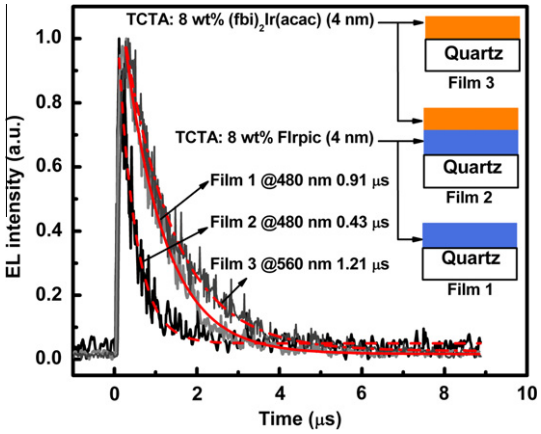

Fig. 4. Transient photoluminescence decay curves of quartz/TCTA: 8 wt.% FIrpic (4 nm) (Film 1), quartz/TCTA: 8 wt.% FIrpic (4 nm)/TCTA: 8 wt.%$(fbi)_2$ Ir(acac) (4 nm) (Film 2) and quartz/TCTA: 8 wt.%$(fbi)_2$Ir(acac) (4 nm) (Film 3).

has a lifetime of 1.21 μs. This lifetime is a little longer than that of FIrpic (0.91 μs). This indicates that even the lifetime of the orange dopant is longer than the blue dopant, there can be energy transfer from the blue dopant to the orange dopant as well.

To further demonstrate the existence of the energy transfer in our double EML white OLED, we studied the influence of the concentration of FIrpic and $(fbi)_2Ir(acac)$ dopants at the interface between blue EML and orange

EML on the EL spectrum. For the case of changing the FIrpic concentration, the used device structures are ITO/MoO_3(10 nm)/NPB(80 nm)/TCTA(5 nm)/TCTA: 6 wt.% $(fbi)_2Ir(acac)$ (5 nm)/TCTA: *x* wt.% FIrpic (1 nm) (*x* = 0, 4, 8, 12)/TCTA: 8 wt.% FIrpic (4 nm)/TPBi(50 nm)/LiF(1 nm)/Al. As shown in Fig. 5, as the concentration of FIrpic increases, the blue emission decreases with respect to the orange emission. This is completely different from the case that if just considering exciton diffusion on TCTA molecules, the blue emission would increase by harvesting more excitons from TCTA in the case of higher FIrpic concentration. For the case of 0 wt.% FIrpic in TCTA, partial excitons will be blocked in the blue EML. As the concentration of FIrpic increases, more excitons can diffuse out the blue EML into the orange EML. The percentage of calculated orange photon number to the total photon number emitted by the white light increases from 51.6% to 58.1% as the FIrpic concentration increases from 0 wt.% to 12 wt.% (see Fig. S5, Supporting information). This means that there does exist an efficient energy transfer from the blue EML to the orange EML, leading amounts of energy formed in blue EML to the orange EML.

Similarly, the influence of $(fbi)_2Ir(acac)$ concentration on EL spectra in double EML white OLED can also prove this point. The used device structures are ITO/MoO_3(10 nm)/NPB(80 nm)/TCTA(5 nm)/TCTA: 6 wt.% $(fbi)_2Ir(acac)$ (4 nm)/TCTA: *x* wt.% $(fbi)_2Ir(acac)$ (1 nm) (*x* = 0, 4, 8, 12)/TCTA: 8 wt.% FIrpic (5 nm)/TPBi(50 nm)/LiF(1 nm)/Al. As shown in Fig. 6, the influence of $(fbi)_2Ir(acac)$ concentration on the emissive spectra is more significant. The percentage of calculated orange photon number to the total photon number emitted by the white light, in this case, increases from 42% to 65% as the $(fbi)_2Ir(acac)$ concentration increases from 0 wt.% to about 12 wt.% (see Fig. S6, Supporting information). The higher the $(fbi)_2Ir(acac)$ concentration is, the larger the orange emission from $(fbi)_2Ir(acac)$ is. Because the exciton recombination is within the blue EML, the much more orange emission with the increase of $(fbi)_2Ir(acac)$ concentration indicates that the $(fbi)_2Ir(acac)$ molecules capture the more excitons from the blue EML. This should

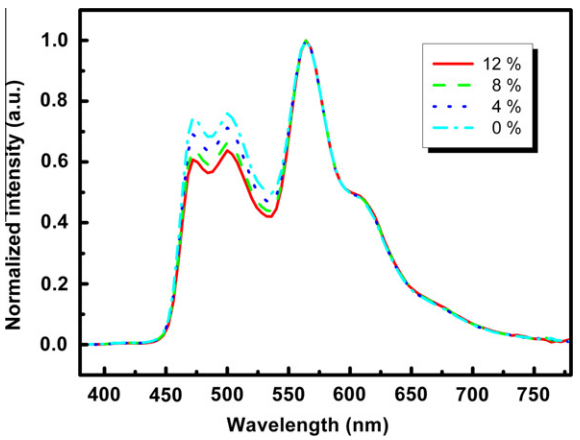

Fig. 5. Effect of FIrpic concentrations on emissive spectra in double EML white OLED measured at 0.4 mA cm^{-2}.

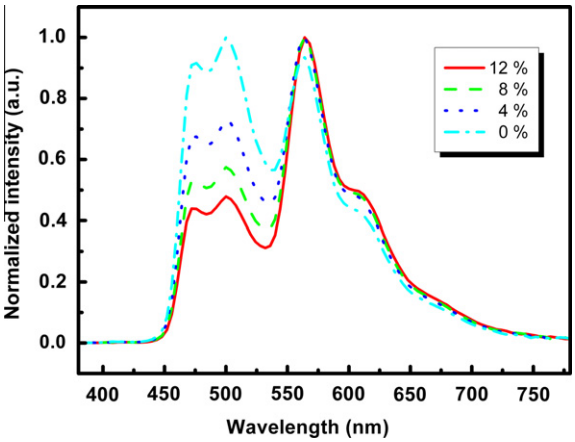

Fig. 6. Effect of $(fbi)_2Ir(acac)$ concentrations on emissive spectra in double EML white OLED measured at 0.4 mA cm^{-2}.

be identical to the spectral variation by changing the concentration of FIrpic.

3.3. Exciton recombination region and its effect

To determine the exciton recombination region within the EML near the ETL in our double EML white OLEDs, we made the following devices where a thin orange emissive layer of 0.05 nm (regarded as δ-OEML), which was called delta-doping method [28–30], is inserted between two blue EMLs [a schematic diagram is shown in the inset of Fig. 7(a)]. The structures of the four devices here are: ITO/MoO_3(10 nm)/NPB(80 nm)/TCTA(5 nm)/TCTA: 8 wt.% FIrpic(10 − *x* nm)/$(fbi)_2Ir(acac)$(0.05 nm)/TCTA: 8 wt.% FIrpic (*x* nm)/TPBi (50 nm)/LiF(1 nm)/Al(150 nm), where *x* = 1, 3, 5 and 7. As shown in Fig. 7(a), the position of the δ-OEML does not affect the J–V characteristics of the devices. This should be favor in the study on the comparison of the optical property in the case of unchanging electrical property in fabricated devices. Fig. 7(b) shows the EL spectra of the 4 devices at a constant current density of 9 mA cm^{-2} with different δ-OEML distances from the EML and the ETL interface. It can be seen that the orange emission intensity decreases gradually and the blue emission increases accordingly with the increase of the δ-OEML distance until the emission shows mainly a blue emission as the δ-OEML distance reaches 7 nm. This means that the exciton recombination region is indeed localized in the blue EML near the interface between blue EML and ETL. Furthermore, as shown in Fig. 7(c–f), it can be seen that the EL spectra are almost unchanged with the increase of bias voltages when the δ-OEML distance is more than 3 nm. This indicates that the orange emission from the $(fbi)_2Ir(acac)$ molecules is completely due to the energy transfer from the excitons near the EML/ETL interface because the spectra should be changed if there exists direct charge carrier trapping on $(fbi)_2Ir(acac)$ molecules. Accordingly, the electron injection depth from the interface between the blue EML and ETL into the blue EML should also less than 3 nm before totally recombining with holes.

We do further study on the exciton recombination zone effect by changing the thickness of blue EML in our double

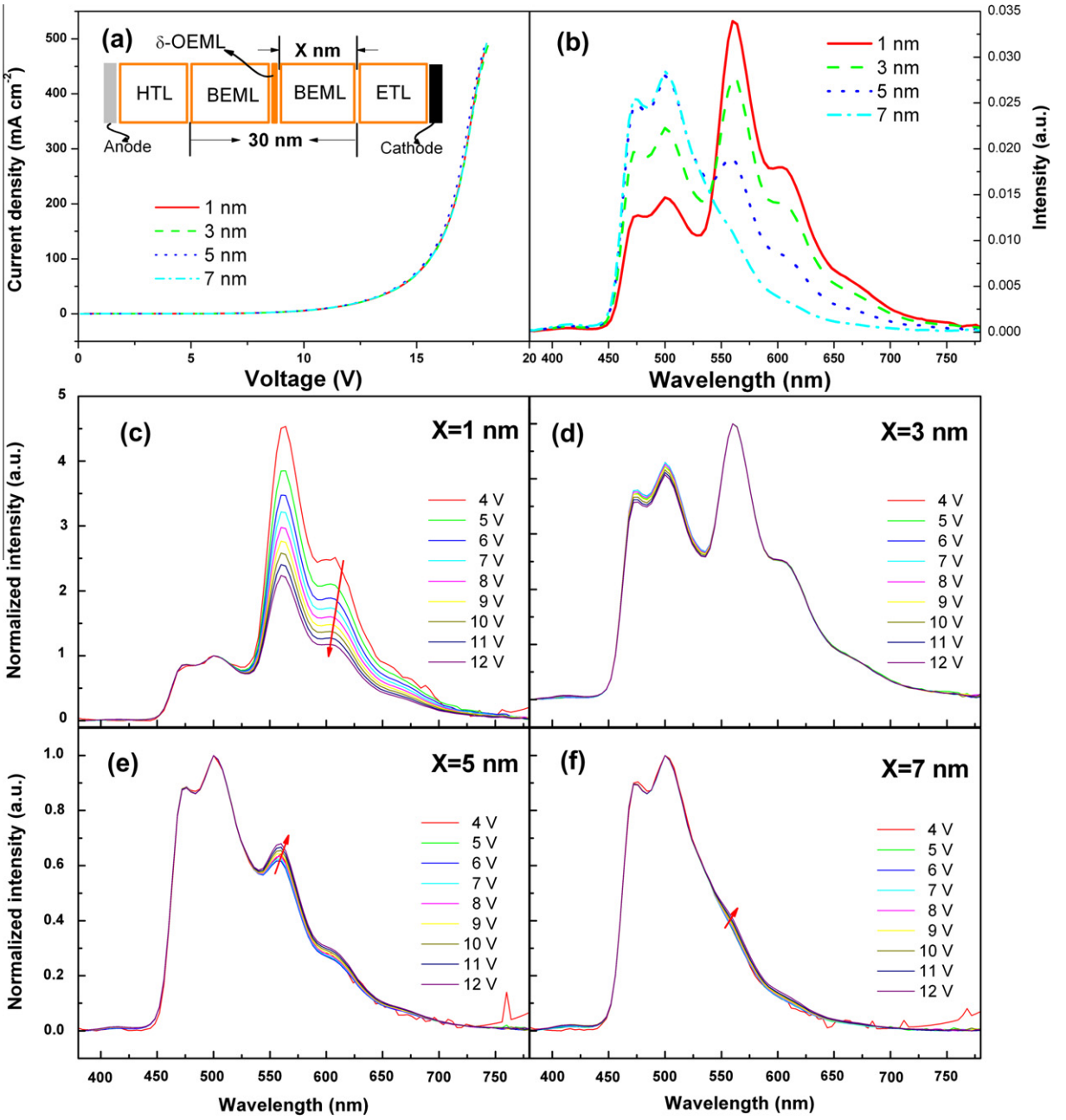

Fig. 7. (a): Current–voltage characteristics of the tested devices and inset shows a schematic view of device structures. (b): Emission spectra of the tested devices with different δ-doped layer distances at constant current density of 9 mA cm^{-2}. (c–f) Emission spectra of the tested devices with different δ-OEML distances at different bias voltages.

EML white OLEDs. The detailed device structures are ITO/MoO_3(10 nm)/NPB(80 nm)/TCTA(5 nm)/TCTA: 6 wt.%$(fbi)_2$Ir(acac)(5 nm)/TCTA: 8 wt.% FIrpic (1, 2, 3 and 4 nm)/TPBi (50 nm)/LiF(1 nm)/Al(150 nm). Fig. 8(a–d) shows the spectra of these white OLEDs with blue EML thicknesses of 1 nm, 2 nm, 3 nm and 4 nm, respectively. It can be clearly seen that the devices with 1 nm and 2 nm blue EML show obvious spectral variation with bias voltages, whereas the devices with 3 nm and 4 nm blue EML almost does not change the spectra at different bias voltages. This further demonstrates that the width of exciton recombination in the blue EML should be less than 3 nm and the electron transport distance in the blue EML should be no more than 3 nm before totally recombining with holes (see Fig. S9, Supporting information). In our double EML white OLEDs, we have used 5 nm thickness of blue EML, which not only avoids the direct electron–hole recombination on the orange dopants, but also guarantees the effective energy transfer from the blue EML to the orange EML across the interface between the blue EML and the orange EML, finally leading to the simultaneous emission of blue and orange light. As a good evidence, all the eight devices used

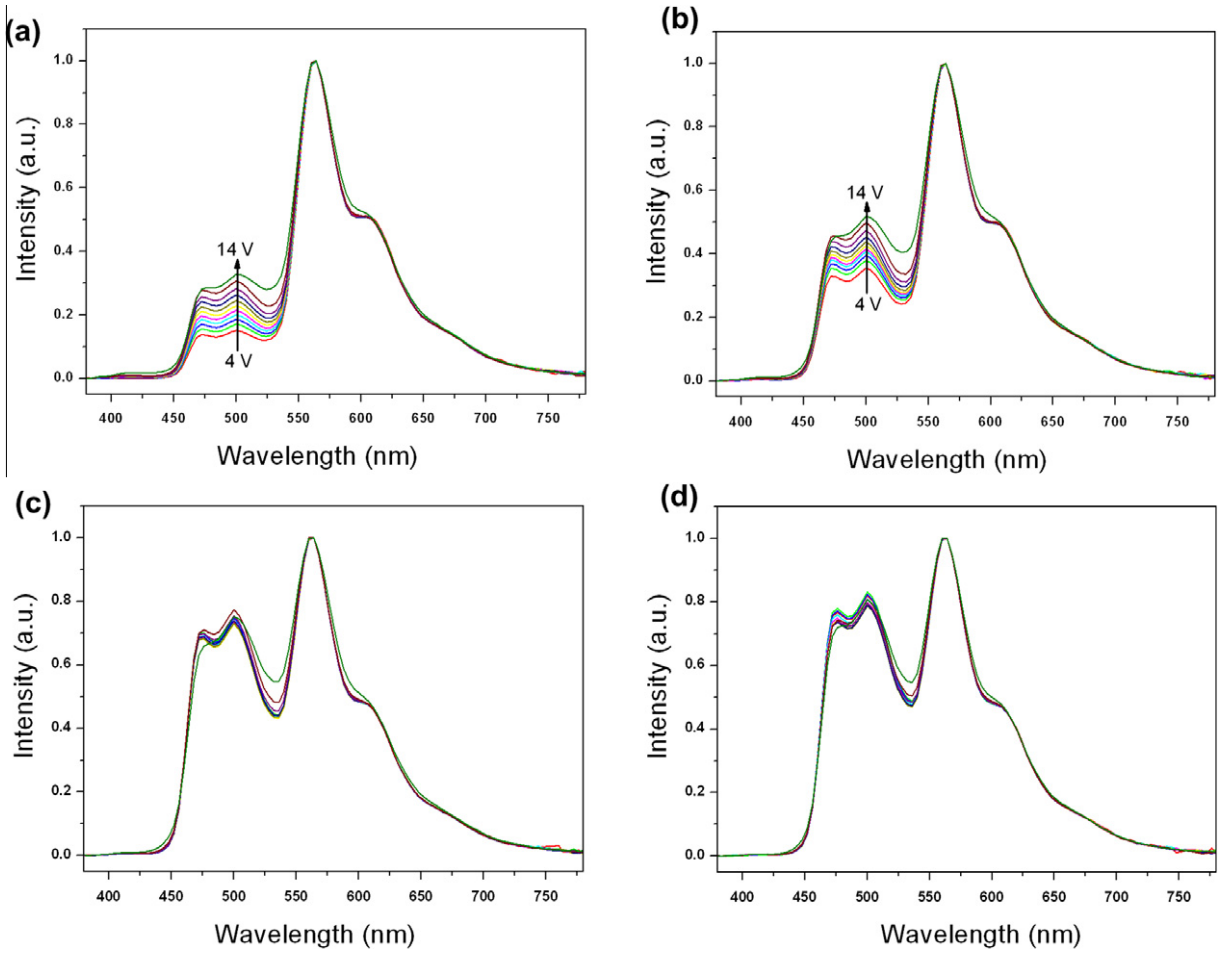

Fig. 8. Influence of blue EML thickness on color stability of double EML white OLEDs.

in Fig. 5 and 6, which have blue EML thickness larger than 3 nm, show very good color stability with driving voltages (see Fig. S7 and S8, Supporting information).

Clearly, the thickness of ETL should also have strong effect on the spectral stability due to the role of ETL in the electron transport. The thinner the ETL is, the deeper the electrons are injected into the blue EML. This means that the thinner ETL will greatly increase the possibility the electrons are injected into the orange EML(see Fig. S10, Supporting information). As stated above, this will lead to a poor spectral stability. As shown in Fig. 9, the emissive color indeed shows more pronounced variation with bias voltage as the thickness of ETL is gradually reduced from 50 nm to 20 nm. This indicates that as the thickness of the ETL decreases to about 30 nm, the electrons will penetrate the blue EML into the orange EML, leading to the direct recombination of holes and electrons on the $(fbi)_2Ir(acac)$ molecules. This further verifies the importance of removing the electrons far from the orange EML.

3.4. Working mechanism

The working processes of our optimized double EML white OLEDs are summarized in Fig. 10. It also is not difficult to see from the energy diagram that the recombination region should be localized in the blue EML near to the interface between the blue EML and the ETL, because, as we know, the utilization of MoO_3 [31–34] interface can greatly enhance the hole injection and TCTA is used

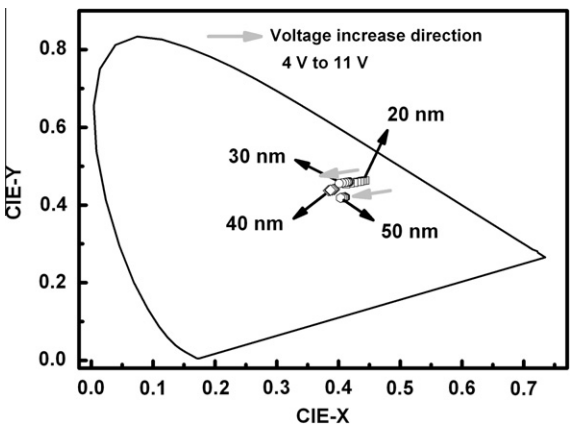

Fig. 9. CIEs variations of double EML white OLEDs with varying ETL thickness (voltage ranges from 4 V to 11 V).

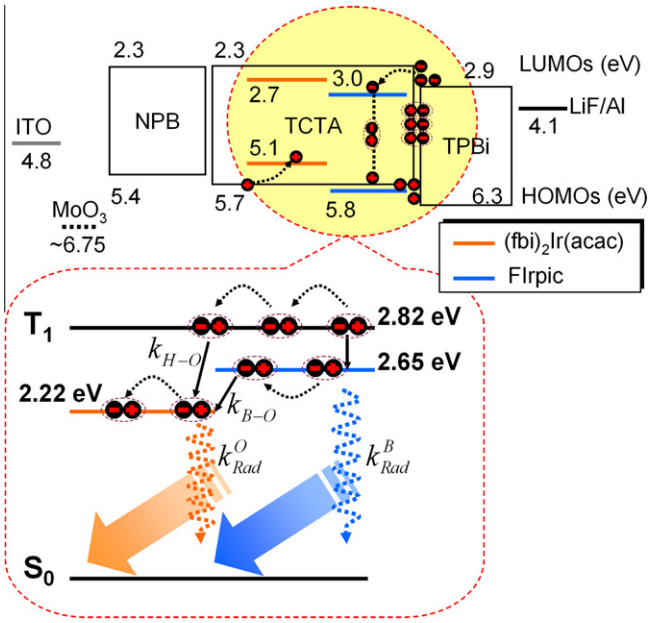

Fig. 10. Proposed energy diagram and exciton dynamics for the optimized double EML white OLEDs.

as host in EML, which generally shows two orders higher of hole mobility than electron mobility [15,24]. In this case, except that the partial holes are trapped by $(fbi)_2Ir(acac)$ molecules in the orange EML, the most of injected holes are transported into the blue EML along TCTA molecules and accumulated at the region near the interface between the blue EML and the ETL. As electrons are injected into the blue EML from cathode, they would recombine with the accumulated holes on TCTA and FIrpic molecules. As we know, the width of the recombination region is about 3 nm. Then the partially formed excitons in the recombination zone will lead to the blue emission, and the partial excitons will diffuse on TCTA and FIrpic molecules, and immigrate into the orange EML across interface between the blue EML and the orange EML, leading to the orange emission by energy transfer. Because the injected electrons cannot be transported into the orange EML, the direct recombination of electrons with the holes trapped on the orange dopant is greatly suppressed, resulting in stable white emission.

It is worthy pointing out that the fabrication of the double EML white OLEDs here is much easier than the multi-doped single EML white OLED counterparts due to the unnecessary of precisely controlling the orange dopant's concentration. It is much easier and practical to get the required color from the double EML white OLEDs by simple thickness adjustments. Moreover, the double EML white OLEDs also show superior color rendition and efficiency roll-off properties.

4. Conclusion

We have systematically investigated the working mechanism of a color stable white OLEDs. The white OLEDs are realized by using a double emissive layers consisted of a blue EML and an orange EML and by controlling the exciton recombination in the blue EML. It can be seen that the direct recombination on orange dopant molecules by charge carrier trapping is greatly suppressed, which is the real reason that leads to the color variation with bias voltage in multi-doped white OLEDs. The orange light emission in our double EML white OLEDs is originated from the energy transfer from the blue EML. Obviously, controlling the position of exciton recombination region is great important in keeping the color stability and realizing high efficiency for the fabrication of white OLEDs.

Acknowledgements

The authors thank the Science Fund for Creative Research Groups of NSFC (20921061), the National Natural Science Foundation of China (50973104, 60906020, 21161160442, 61036007), Ministry of Science and Technology of China (973 program No. 2009CB623604, 2009CB930603), the Foundation of Jilin Research Council (20090127, 201105028) for the support of this research.

Appendix A. Supplementary data

Supplementary data associated with this article can be found, in the online version, at http://dx.doi.org/10.1016/j.orgel.2012.04.015.

References

[1] C.W. Tang, S.A. VanSlyke, Appl. Phys. Lett. 51 (1987) 913–915.
[2] B.W. D'Andrade, S.R. Forrest, Adv. Mater. 16 (2004) 1585–1595.
[3] S.R. Forrest, Org. Electron. 4 (2003) 45–48.
[4] F. So, J. Kido, P. Burrows, MRS Bull. 33 (2008) 663–669.
[5] Q. Wang, D. Ma, Chem. Soc. Rev. 39 (2010) 2387–2398.

[6] P.A. Levermore, V. Adamovich, K. Rajan, W. Yeager, C. Lin, S. Xia, G.S. Kottas, M.S. Weaver, R. Kwong, R. Ma, M. Hack, J.J. Brown, SID Symp. Digest 41 (2010) 786–789.
[7] S. Reineke, F. Lindner, G. Schwartz, N. Seidler, K. Walzer, B. Lussem, K. Leo, Nature 459 (2009) 234–238.
[8] F.C. Chen, S.C. Chien, Y.S. Chen, Appl. Phys. Lett. 94 (2009) 043306.
[9] B.D. Chin, M.C. Suh, M.-H. Kim, S.T. Lee, H.D. Kim, H.K. Chung, Appl. Phys. Lett. 86 (2005) 133505.
[10] M.-T. Lee, J.-S. Lin, M.-T. Chu, M.-R. Tseng, Appl. Phys. Lett. 93 (2008) 133306.
[11] F. Nüesch, D. Berner, E. Tutiš, M. Schaer, C. Ma, X. Wang, B. Zhang, L. Zuppiroli, Adv. Funct. Mater. 15 (2005) 323–330.
[12] K.K. Tsung, S.K. So, Appl. Phys. Lett. 92 (2008) 103315.
[13] S. Ishihara, T. Okachi, H. Naito, Thin Solid Films 518 (2009) 452–456.
[14] Q. Wang, J. Ding, D. Ma, Y. Cheng, L. Wang, X. Jing, F. Wang, Adv. Funct. Mater. 19 (2009) 84–95.
[15] R.J. Holmes, B.W. D'Andrade, S.R. Forrest, X. Ren, J. Li, M.E. Thompson, Appl. Phys. Lett. 83 (2003) 3818–3820.
[16] Y. Luo, H. Aziz, Adv. Funct. Mater. 20 (2010) 1285–1293.
[17] M.C. Gather, R. Alle, H. Becker, K. Meerholz, Adv. Mater. 19 (2007) 4460–4465.
[18] Q. Wang, J. Ding, D. Ma, Y. Cheng, L. Wang, Appl. Phys. Lett. 94 (2009) 103503.
[19] Q. Wang, J. Ding, D. Ma, Y. Cheng, L. Wang, F. Wang, Adv. Mater. 19 (2009) 2397–2401.
[20] Q. Wang, C.-L. Ho, Y. Zhao, D. Ma, W.-Y. Wong, L. Wang, Org. Electron. 11 (2010) 238–246.
[21] K.S. Yook, S.O. Jeon, C.W. Joo, J.Y. Lee, Appl. Phys. Lett. 93 (2008) 073302.
[22] C.-H. Hsiao, Y.-H. Lan, P.-Y. Lee, T.-L. Chiu, J.-H. Lee, Org. Electron. 12 (2011) 547.
[23] M. Hoping, C. Schildknecht, H. Gargouri, T. Riedl, M. Tilgner, H.H. Johannes, W. Kowalsky, Appl. Phys. Lett. 92 (2008) 213306.
[24] J.-W. Kang, S.-H. Lee, H.-D. Park, W.-I. Jeong, K.-M. Yoo, Y.-S. Park, J.-J. Kim, Appl. Phys. Lett. 90 (2007) 223508.
[25] J. Lee, J.-I. Lee, K.-I. Song, S.J. Lee, H.Y. Chu, Appl. Phys. Lett. 92 (2008) 133304.
[26] B. D'Andrade, R. Holmes, S. Forrest, Adv. Mater. 16 (2004) 624–628.
[27] M.A. Baldo, C. Adachi, S.R. Forrest, Phys. Rev. B 62 (2000) 10967–10977.
[28] H. Choukri, A. Fischer, S. Forget, S. Chenais, M.-C. Castex, D. Ades, A. Siove, B. Geffroy, Appl. Phys. Lett. 89 (2006) 183513.
[29] C.W. Tang, S.A. VanSlyke, C.H. Chen, J. Appl. Phys. 65 (1989) 3610–3616.
[30] T. Tsuji, S. Naka, H. Okada, H. Onnagawa, Appl. Phys. Lett. 81 (2002) 3329–3331.
[31] Irfan, H. Ding, Y. Gao, C. Small, D.Y. Kim, J. Subbiah, F. So, Appl. Phys. Lett. 96 (2010) 243307.
[32] T. Matsushima, G.-H. Jin, H. Murata, J. Appl. Phys. 104 (2008) 054501.
[33] T. Shizuo et al., J. Phys. D Appl. Phys. 29 (1996) 2750.
[34] H. You, Y. Dai, Z. Zhang, D. Ma, J. Appl. Phys. 101 (2007) 026105.